# Lanthanide Oxides: Preparation and Ageing †

**Rafael Alvero, Jose A. Odriozola, and Jose M. Trillo** *
*Department of Inorganic Chemistry, Faculty of Pharmacy, University of Seville, Seville, Spain*
**Serafin Bernal**
*Department of Inorganic Chemistry, Faculty of Chemistry, University of Cádiz, Cádiz, Spain*

$La_2O_3$, $CeO_2$, $Sm_2O_3$, $Dy_2O_3$, and $Yb_2O_3$ were obtained by calcining in air phases prepared by precipitation with ammonia from solutions of the corresponding nitrates. During the calcination to oxides, under the experimental conditions used, the nitrate ions are removed to an extent which could not be detected by temperature programmed desorption–mass spectrometry or i.r. spectroscopy, contradictory to the established literature. For comparative purposes, $Yb_2O_3$ has also been prepared by thermal decomposition of oxalate. The Brunauer–Emmett–Teller surface area was always lower for the oxide obtained from oxalate. This was so even after thermal treatment at 1 173 K. Independent of the preparation method, the heaviest 4*f* oxides undergo partial conversion to bulk carbonate hydroxides when exposed to air. According to our results and those reported in the literature, lanthanide oxides, when used as catalysts, are often activated at temperatures lower than those necessary for the complete elimination of $CO_2$ and $H_2O$.

Investigations of lanthanide oxide interaction with atmospheric $H_2O$ and $CO_2$ have primarily dealt with the earlier members of the 4*f* series,[1,2] being currently rather fragmentary and incomplete.

Although recently criticised,[3] the chemistry of lanthanide elements is traditionally considered to be determined by the lanthanide contraction effect. In accordance with this, several authors [2,4] have suggested that bulk hydration in air of 4*f* oxides is only important for the earlier members of the series, being unfavoured from $Gd_2O_3$ onwards.

In the present paper some data from a systematic investigation of the reactivity of 4*f* oxides towards $CO_2$ and $H_2O$, under atmospheric conditions, are reported. Five representative lanthanide oxides, $La_2O_3$, $CeO_2$, $Sm_2O_3$, $Dy_2O_3$, and $Yb_2O_3$, have been studied. The influence of the preparation method has been investigated, particularly the existence of occluded nitrate ions in the oxides prepared and the likely effect on their reactivity of these foreign ions. Regarding hydration and carbonation phenomena, our results have shown, contrary to reports in the literature, that even the heaviest 4*f* oxides undergo these processes in bulk. On the other hand, it can also be deduced from our data that, when used as catalysts, these oxides are often activated at temperatures lower than those necessary to achieve the complete elimination of $CO_2$ and $H_2O$. Finally, the influence on the textural properties of these oxides of exposure to the air and several regeneration thermal treatments is reported.

## Experimental

*Materials.*—$La_2O_3$, $CeO_2$, $Sm_2O_3$, $Dy_2O_3$, and $Yb_2O_3$ were obtained by calcining in air, at 873 K, phases previously prepared by precipitation with ammonia (1 mol $dm^{-3}$) from the corresponding nitrate solution. The ammonia was added at a rate of 5 $cm^3$ $min^{-1}$, under atmospheric $CO_2$, at room temperature. The precipitates were thoroughly washed with boiling water before drying at 383 K.

For comparative purposes, standard commercial samples of the same oxides (Merck A.R. grade) were also used; the numbers (I) and (II) after the lanthanide oxides ($Ln_2O_3$) refer to commercial and prepared oxides, respectively.

A third kind of ytterbium oxide, $Yb_2O_3$ (III), prepared by thermal decomposition of oxalate, has also been studied. The oxalate was homogeneously precipitated at 333—348 K by adding a dimethyl oxalate solution to the 99.9% pure commercial oxide dissolved in 0.2 mol $dm^{-3}$ $HNO_3$. The hydrated oxalate was heated in air at 873 K for 6 h.

Finally, in order to prepare ytterbium carbonate hydroxide, which was further used as a reference sample, the procedure reported in ref. 5 was followed.

*Apparatus.*—Thermogravimetric analyses (t.g.a.) were made with a Cahn RG electrobalance in a conventional vacuum system. For differential thermal analysis (d.t.a.) experiments, an Aminco 4.4442 thermoanalyzer with alumina as reference was used.

Details concerning the temperature programmed desorption (t.p.d.) device, in which gas chromatography (t.p.d.–g.c.) and mass spectrometry (t.p.d.–m.s.) were used as analytical techniques, are given elsewhere.[6] The heating rate was always 8 K $min^{-1}$.

*X*-Ray powder diffraction diagrams were obtained with a Phillips PW 1060 instrument, using Cu-$K_\alpha$ radiation and a Ni filter. The *X*-ray photoelectron spectra (x.p.s.) were recorded on a McPherson ESCA 36 instrument, using Mg-$K_\alpha$ radiation. The observed line positions were corrected by comparing the C(1*s*) signal of the sample to that of Au. The spectra were analysed using the deconvolution method previously reported.[7]

Infrared spectra were recorded on a Perkin-Elmer 577 spectrometer. Self-supported discs with a density of 20—30 mg $cm^{-2}$ and 18 mm diameter, prepared by compressing the powdered samples at 5 000 kg $cm^{-2}$, were used. The samples were studied in a vacuum cell.[8]

Scanning electron micrographs were obtained by covering the oxide samples with Au in a Hitachi HHS-2R instrument.

The pore size distribution measurements were made employing spectroscopically pure nitrogen at 77 K.

## Results and Discussion

Figure 1 shows thermograms of La, Sm, Dy, and Yb phases, obtained by precipitation with ammonia from the corresponding nitrate solutions as described above. These phases, of the carbonate hydroxide type in accordance with the analysis of evolved gases, were amorphous. From t.g.a. data, $CO_2$ : $Ln_2O_3$ mol ratios ranging from *ca.* 2 (Ln = La and Sm) to *ca.* 1.5 (Ln = Dy and Yb) have been found. Precipitation

---

† *Non-S.I. units employed*: 1 Torr = (101 325/760) Pa; 1 eV = 1.60 × $10^{-19}$ J.

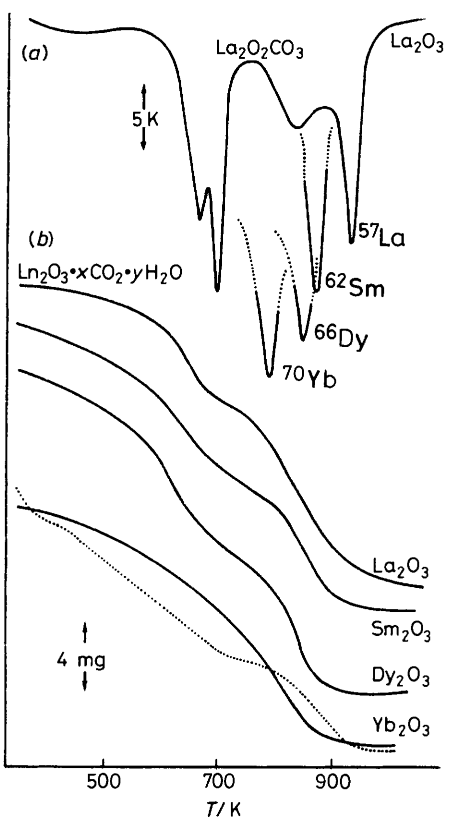

Figure 1. Thermal evolution of phases prepared by precipitation with ammonia from nitrate solutions: d.t.a. (*a*) and t.g. (*b*) curves corresponding to La, Sm, Dy, and Yb phases. Dotted t.g. diagram is for ytterbium carbonate hydroxide (obtained as reported in ref. 5), for comparison

with ammonia under atmospheric $CO_2$ (30 Pa) invariably produces amorphous carbonate hydroxides of variable composition.[9-11] Crystalline phases require hydrothermal synthesis at drastic pressures (up to $1.4 \times 10^8$ Pa) and temperatures (up to 1 100 K).[12-14] The results above suggest that the thermal decomposition of the carbonate hydroxides takes place through the corresponding carbonate dioxides, $Ln_2O_2CO_3$, a species already reported as intermediate in the decomposition of a number of 4*f* salts.[15] The temperatures at which the two complex decomposition stages are observed decrease as the polarizing power of the 4*f* ions increases. For the first stage the temperature range is 648—603 K, and for the second, 938—793 K.

During the final step to $Ln_2O_3$ the evolution of nitrogen oxides could be observed. Precipitation with ammonia from solutions of rare-earth nitrates, chlorides, or sulphates occludes amounts of these ions. This can affect both the decomposition profile of the precipitate [12] and the surface properties of the final oxides.[2] In a relatively recent review [16] it is reported that such ions are present in the oxides to such an extent as to modify their catalytic behaviour. Accordingly, the above preparation method is generally avoided.

The thermogram for the cerium precipitate, different from those previously reported, is consistent with the decomposition to $CeO_2$ of a tetrahydroxide almost free of carbonate.

As is known, t.g.a. and d.t.a. experiments do not take place under true equilibrium conditions, so that, at the limit of zero heating rate, the decomposition stages are initiated at lower temperatures. Accordingly, additional experiments were made in which the samples were decomposed at several increasing temperatures. The final solid phases were identified by *X*-ray diffraction and their Brunauer–Emmett–Teller (B.E.T.) surface areas determined. From this study, the temperature of 873 K was selected to decompose all the carbonate hydroxides to oxides [series (II)]. In this way, well defined oxide phases with rather high surface areas could be obtained.

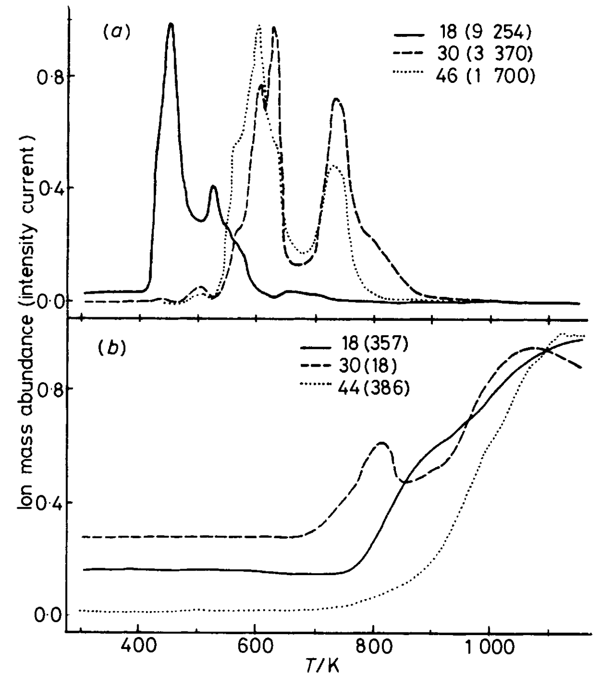

Figure 2. T.p.d.–m.s. experiments corresponding to (*a*) decomposition of $Yb(NO_3)_3 \cdot 5H_2O$ and (*b*) evolution of $Yb_2O_3$ (II) previously heated in He flow at 823 K. Data in brackets account for the full scale range in which the corresponding *m*/*e* signals were recorded

According to our t.p.d. and i.r. spectroscopy data, the above reported method allows the preparation of oxides almost completely free of nitrate. Figure 2 shows t.p.d. diagrams corresponding to the decomposition of $Yb(NO_3)_3 \cdot 5H_2O$, a reference sample, and $Yb_2O_3$ (II) aged two years in air and heated for 4 h in a flow of He at 823 K; this activation treatment has been used previously.[17,18] As can be seen in Figure 2(*b*), for $Yb_2O_3$ (II), no signal corresponding to $NO_2^+$ ($m/e = 46$) could be detected. Likewise, the trace for $m/e = 30$ ($NO^+$) is plotted on a full scale of 18 units whereas for the reference sample, Figure 2(*a*), the range of 3 370 units for the full scale should be used. Taking into account the contribution of $C^{18}O^+$ to the signal at $m/e = 30$, a concentration of nitrate ion in $Yb_2O_3$ (II) lower than 20 p.p.m. can be estimated.

Because of their basicity, a combination of rare-earth oxides with atmospheric $H_2O$ and $CO_2$ would be expected. However, it is generally accepted that bulk hydration of the heaviest oxides is not favoured.[2,4] As the experimental basis of the last statement is inadequate, the transformation of series (I) and series (II) oxides, exposed to the air up to three years, has been studied. Samples of each oxide were examined by *X*-ray diffraction, x.p.s. and thermal analysis.

The diffraction pattern for a $La_2O_3$ sample recently prepared showed the coexistence of the hexagonal phase of the oxide as well as the corresponding hydroxide. All the other $Ln_2O_3$ oxides showed type C (cubic) structure, except $Sm_2O_3$ (I). For this sample, monoclinic (B) and C phases could be detected, which suggests a calcination temperature around 1 175 K for $Sm_2O_3$ (I). The diffraction patterns for both $CeO_2$ (I) and (II) correspond to a fluorite-like structure. Exposure of oxides to the air for up to three years only causes the increase of diffraction lines attributable to the hydroxides

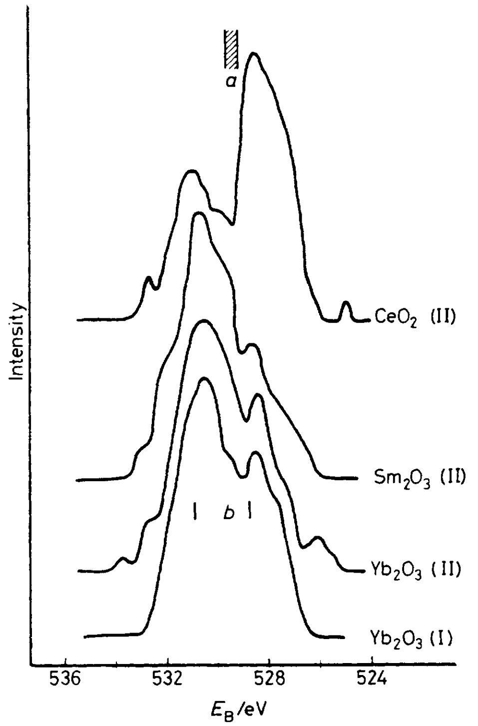

**Figure 3.** X.p.s. data for O(1*s*) binding energies; see text for definition of *a* and *b*

in $La_2O_3$ (I) and (II) and $Sm_2O_3$ (I) and (II). For the remaining oxides only a widening of the original peaks is observable. In the cases of $Dy_2O_3$ and $Yb_2O_3$ hydroxide lines have not been observed either. It is worth mentioning, however, that several amorphous phases have been reported for the $Ln_2O_3$–$CO_2$–$H_2O$ system.

X.p.s. spectra of the oxides exposed to air are reported in Figure 3. According to previous studies [19,20] the principal peaks at 528.5, 530.5, and 532.5 eV can be assigned to oxide, hydroxide, and carbonate species respectively. Noller and co-workers [21] have proposed the existence of a direct relationship between effective basic strength and O(1*s*) binding energy in oxides. In the present case, however, no systematic shift of the corresponding signal is observed; only the distribution of electron-pair donor centres changes with the nature of cation and the method of preparation. The smooth pattern reported [22] for the variation of O(1*s*) binding energies throughout the whole series of 4*f* $Ln_2O_3$ oxides falls in the shaded range (*a*) shown in Figure 3. On the other hand, the intensity ratio of peaks at 530.5 and 528.5 (range *b*) is 1.4, which is consistent with bulk hydration of the oxide.[19]

The reaction of $Ln_2O_3$ with atmospheric $CO_2$ and $H_2O$ was quantitatively studied by t.g.a. As an example, Figure 4 shows t.g.a. traces for the lightest and heaviest oxides of the series, aged two years in air. The decomposition profile is the same for each oxide, irrespective whether the samples are of series (I) or (II). Data concerning the intensity of the process are given in Table 1. Differences between surface areas of series (I) and (II) oxides might well account for the differences found in Table 1. From the total weight loss it can be concluded that bulk hydration–carbonation occurs even for $Yb_2O_3$. Although the decomposition stages overlap, from simultaneous gas chromatographic analysis of evolved gases the loss of $H_2O$, together with some $CO_2$, followed by the elimination of $CO_2$ could be observed. The final step is only completed at temperatures ranging from 1 000 K for $La_2O_3$ to 900 K for $Yb_2O_3$.

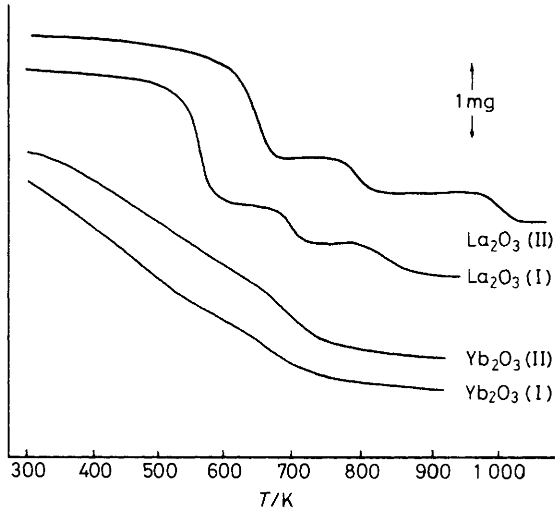

**Figure 4.** Thermograms for $La_2O_3$ and $Yb_2O_3$ exposed to air for two years. In the case of $Yb_2O_3$ (I) the ordinate scale is expanded 7 times

**Table 1.** T.g.a. data for $Ln_2O_3$ aged two years in air

| Oxide | Weight loss (%) (I) | Weight loss (%) (II) |
|---|---|---|
| $La_2O_3$ | 13.4 | 14.0 |
| $Sm_2O_3$ | 2.2 | 7.8 |
| $Dy_2O_3$ | 2.1 | 8.3 |
| $Yb_2O_3$ | 0.8 | 5.1 |

The decomposition pattern described above is similar to the one observed for a carbonate hydroxide phase prepared by us for comparison, Figure 5.

These results lead to the conclusion that all 4*f* $Ln_2O_3$ oxides here studied, even the heaviest ones, undergo partial conversion to carbonate hydroxides when exposed to air. The final decomposition temperatures are higher than those corresponding to phases precipitated from aqueous nitrates. These high decomposition temperatures create a serious difficulty, since 4*f* oxides, when used as catalysts, are often activated at temperatures lower than those necessary to achieve the complete elimination of $H_2O$ and $CO_2$.[23-25]

Additional details of the dehydration–decarbonation process were obtained by i.r. spectroscopy. For a sample of $Yb_2O_3$ (II), exposed to the air, the most notable features are found at 3 650 $cm^{-1}$ as well as in the range 1 700—1 200 $cm^{-1}$. The former band may be assigned to the stretching of isolated hydroxide ions. On the other hand, the presence of carbonate species and molecular water might well account for the broad bands observed in the region 1 700—1 200 $cm^{-1}$. According to the successive thermal treatments *in vacuo*, the elimination of $H_2O$ seems to be almost complete at 500 K. On the contrary, the sample is free of carbonate at temperatures as high as 900 K. At each of the studied temperatures between 383 and 1 073 K, the sample was evacuated at $10^{-6}$ Torr until constant spectra were obtained.

The influence of the hydration and carbonation phenomena on the texture of oxides was examined by scanning electron microscopy (s.e.m.) and $N_2$ adsorption at the temperature of liquid nitrogen. From s.e.m. pictures (Figure 6) a strong effect on the surface can be observed. The micrographs at 5 000 (*a*, *c*, *d*) and 2 500 (*b*) magnifications correspond to the

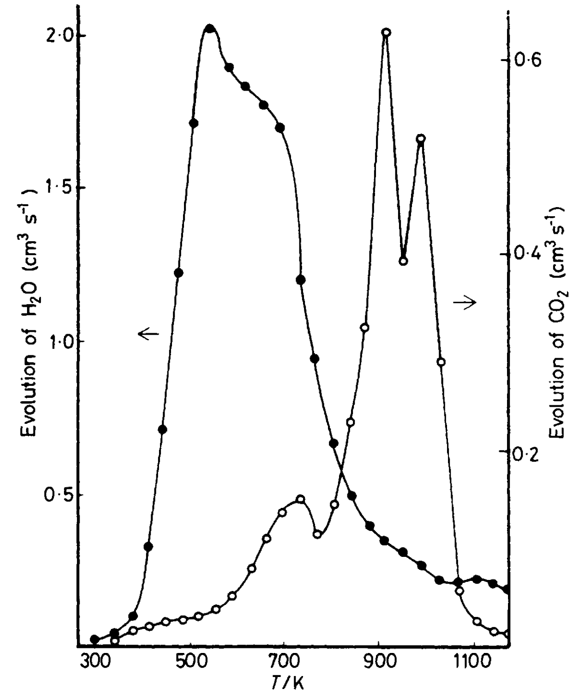

**Figure 5.** T.p.d.-g.c. diagram for ytterbium carbonate hydroxide prepared as reported in ref. 5

**Table 2.** Specific surface area ($m^2\ g^{-1}$) of $Ln_2O_3$ and $CeO_2$

| Oxide | $S_{B.E.T.}$ | $S_\alpha$ | $S_{cum.}$* |
|---|---|---|---|
| $La_2O_3$ | 15 | 15 | 16 |
| $CeO_2$ | 29 | 28 | 37 |
| $Sm_2O_3$ | 25 | 22 | 26 |
| $Dy_2O_3$ | 25 | 26 | 29 |
| $Yb_2O_3$ | 54 | 56 | 55 |

* $S_{cum.}$ = cumulative surface area.

precipitated ytterbium carbonate hydroxide (*a*) and three $Yb_2O_3$ samples (*b*, *c*, *d*). Micrograph (*d*) deals with a recently prepared sample, whereas (*c*) and (*b*) correspond to oxides of series (I) and (II) respectively aged two years in air. The correlation of these results with t.g.a. data is apparent.

Nitrogen isotherms, at 77 K, for oxides of series (II) exposed to air and after the elimination of $CO_2$ and $H_2O$ were also drawn. The first oxides of the series give apparently constant isotherms after periods ranging from a few weeks ($La_2O_3$) to a few months ($Yb_2O_3$). The isotherms were of B.D.D.T. (Brunauer–Deming–Deming–Teller) types II and IV [26] and exhibited hysteresis loops of type A in de Boer's classification. Using a $Yb_2O_3$ sample heated at 1 300 K as reference solid, Sing's α-method [27] showed the absence of micropores; $S_\alpha$ values given in Table 2 were calculated from the slopes of α-plots. Good agreement between $S_\alpha$ and $S_{B.E.T.}$ values is found. The pore size distributions were estimated applying de Boer's method and the experimental multi-layer statistical thickness of the above mentioned reference solid. $La_2O_3$ shows the principal pores within the radius range 90—420 Å, whereas for ytterbia the range was 16—40 Å. The remaining oxides fell between these two limit distributions, Figure 7. Table 2 gives the corresponding cumulative surface area data. The observed discrepancy for $CeO_2$ may derive from a specificity for nitrogen adsorption different from $Ln_2O_3$.

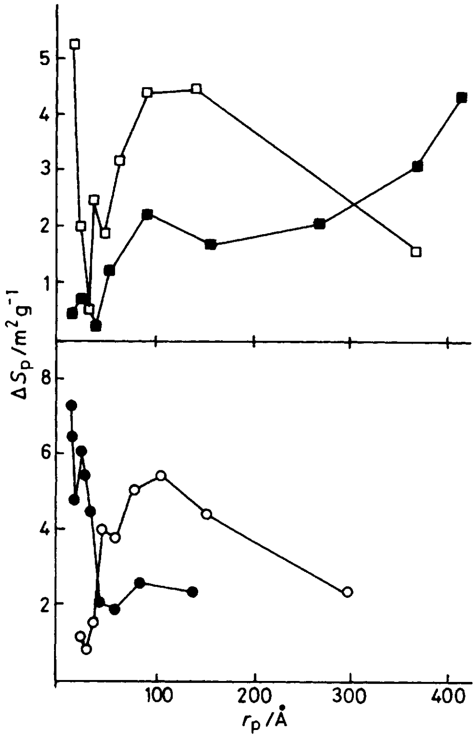

**Figure 7.** Pore size ($r_p$) distribution for $La_2O_3$ (■), $Sm_2O_3$ (□), $Dy_2O_3$ (○), and $Yb_2O_3$ (●) ($\Delta S_p$ is the contribution to the cumulative surface area from pores of mean radius $r_p$)

**Table 3.** Specific surface area of $Yb_2O_3$ (I), (II), and (III) evacuated at various temperatures

| Oxide | T/K | | |
|---|---|---|---|
| | 383 | 823 | 1 173 |
| $Yb_2O_3$ (I) | 7.6 | 7.9 | 8.0 |
| $Yb_2O_3$ (II) | 54 | 58 | 22 |
| $Yb_2O_3$ (III) | 19 | 24 | 4.3 |

The specific surface areas and pore size distribution show small changes with the evacuation of the oxides at temperatures up to *ca.* 850 K. At higher temperatures $S_{B.E.T.}$ values decrease drastically and the pore size distributions become very smooth. However, even after treatment at 1 173 K, $S_{B.E.T.}$ values for oxides of series (II) are higher than those corresponding to oxides prepared by other methods, even when the latter oxides are calcined at lower temperatures. This is illustrated in Table 3, where data for $Yb_2O_3$ (I), (II), and (III), after evacuation for 2 h at the indicated temperatures, are compared.

## Conclusions

Precipitation with ammonia from solutions of rare-earth nitrates implies occlusion of this anion, as stated in the literature.[12,16] However, during calcination to oxide under the conditions here described, the nitrates are removed to an extent as to be considered insignificant by t.p.d.-m.s. or i.r. spectroscopy.

The heaviest 4*f* metal oxides undergo partial conversion to bulk carbonate hydroxides, when exposed to air. The temperatures at which $Ln_2O_3$ catalysts are activated are frequently

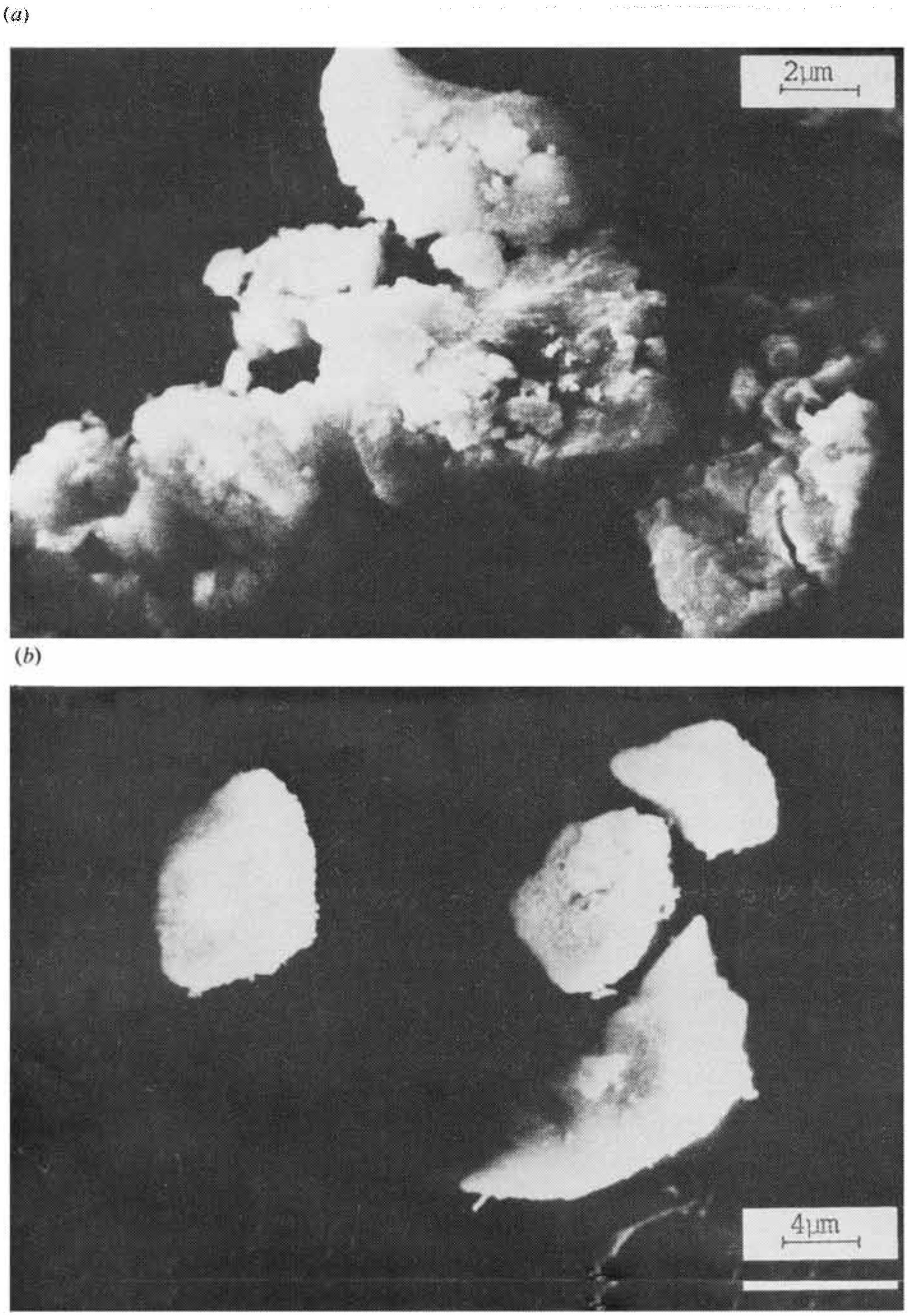

**Figure 6.** S.e.m. micrographs corresponding to (*a*) ytterbium carbonate hydroxide, (*b*) $Yb_2O_3$ (II) exposed to air for two years, (*c*) $Yb_2O_3$ (I) exposed to air for two years, and (*d*) $Yb_2O_3$ (II) recently prepared

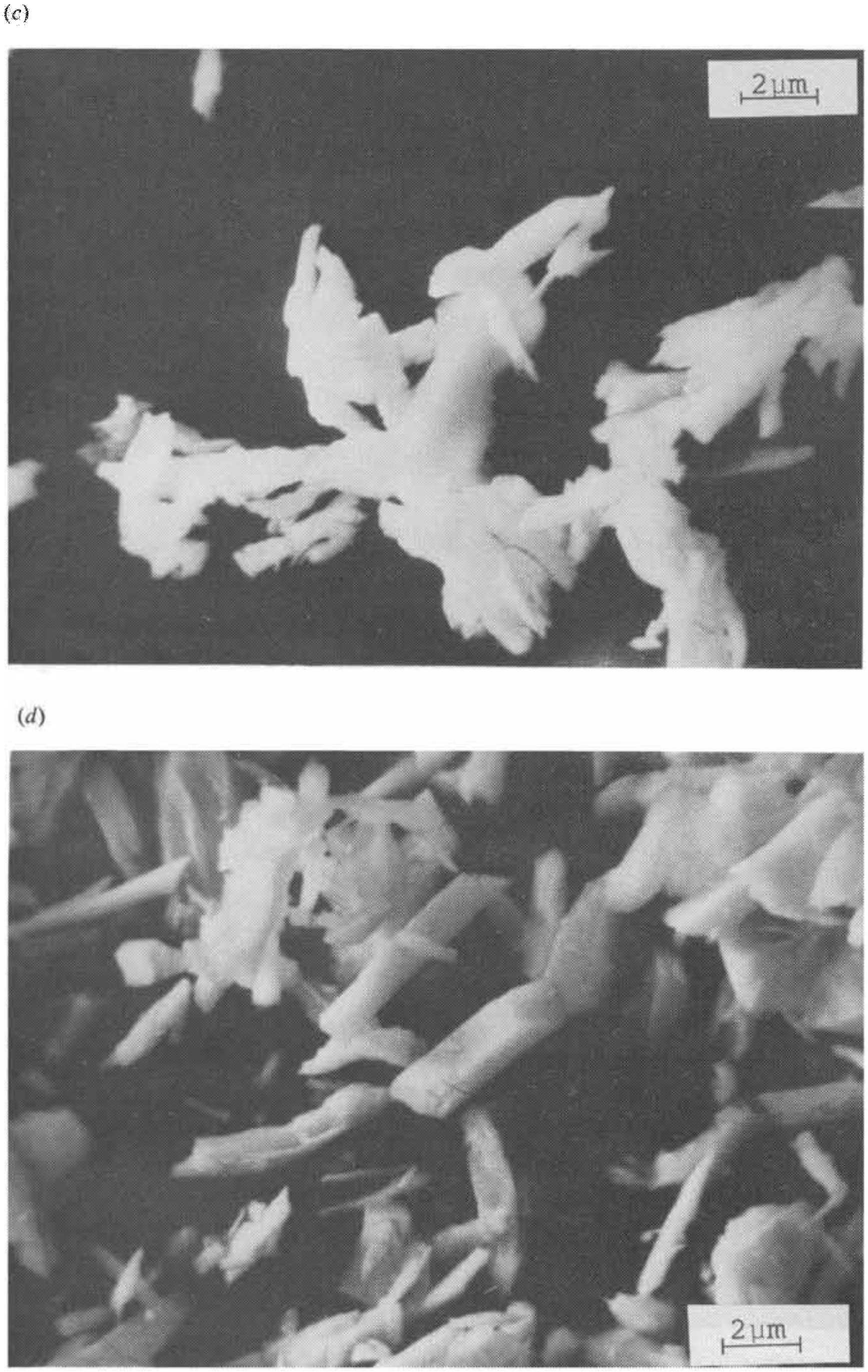
(c)
2 µm
(d)
2 µm

lower than that necessary for the complete elimination of $H_2O$ and $CO_2$.

B.E.T. surface areas of $Ln_2O_3$, prepared by calcination of phases precipitated with ammonia from the corresponding nitrates, are higher, even after thermal treatment at 1 173 K, than those of oxides prepared by oxosalt decomposition.

## References

1 M. P. Rosynek and D. T. Magnuson, *J. Catal.*, 1977, **49**, 285.
2 H. T. Fullam and F. P. Roberts, U.S. Atomic Energy Commission, Report AT(45-1)-1830, 1970, p. 1.
3 D. A. Johnson, *Adv. Inorg. Chem. Radiochem.*, 1977, **20**, 1.
4 D. Touret and F. Queyroux, *Rev. Chim. Miner.*, 1972, **9**, 883.
5 R. G. Charles, *J. Inorg. Nucl. Chem.*, 1965, **27**, 1489.
6 S. Bernal, R. García, and J. M. Trillo, *React. Kinet. Catal. Lett.*, 1979, **10**, 125.
7 M. F. Ebel and N. Gurker, Proc. 7th Int. Vacuum Congress and 3rd Int. Conf. Solid Surf., Vienna, 1977, p. 2249.
8 S. Bernal, C. Blanco, and J. M. Trillo, *Ann. Quim., Suppl. 1*, 1978, **74**, 56.
9 P. E. Caro and M. Lamaitre-Blaise, *C.R. Acad. Sci., Ser. C*, 1969, **269**, 687.
10 H. Dexpert, M. Lamaitre-Blaise, and P. E. Caro, Proc. 7th Int. Congress React. Solids, ed. J. S. Anderson, Chapman and Hall, London, 1972, p. 758.
11 P. E. Caro, J. O. Sawyer, and L. Eyring, *Spectrochim. Acta, Part A*, 1972, **28**, 1167.
12 M. N. Viswanathiah, J. A. K. Tareen, and T. R. N. Kutty, *Indian Mineral.*, 1976, **17**, 54.
13 J. A. K. Tareen, M. N. Viswanathiah, and K. V. Krishnamurthy, *Rev. Chim. Miner.*, 1980, **17**, 50.
14 J. A. K. Tareen and T. R. N. Kutty, *J. Cryst. Growth*, 1980, **50**, 527.
15 I. S. Shaplygin, V. P. Komarov, and V. B. Lazarev, *J. Therm. Anal.*, 1979, **15**, 215.
16 M. P. Rosynek, *Catal. Rev.*, 1977, **16**, 111.
17 S. Bernal and J. M. Trillo, *J. Catal.*, 1980, **66**, 184.
18 S. Bernal, C. Blanco, R. García, A. M. Oliván, and J. M. Trillo, *J. Catal.*, 1981, **71**, 21.
19 B. D. Padalia, J. K. Gimzewski, S. Affrossman, W. C. Lang, L. M. Watson, and D. J. Fabian, *Surf. Sci.*, 1976, **61**, 468.
20 B. D. Padalia and W. C. Lang, *Indian J. Phys., Sect. A*, 1978, **52**, 463.
21 H. Vinek, H. Noller, M. Ebel, and K. Schwarz, *J. Chem. Soc., Faraday Trans. 1*, 1977, 734.
22 V. I. Nefedov, D. Gati, B. F. Dzhurinskii, N. P. Sergushin, and Y. V. Salyn, *Russ. J. Inorg. Chem.* (*Engl. Transl.*), 1975, **20**, 1279.
23 D. R. Ashmead, D. D. Eley, and R. Rudham, *J. Catal.*, 1964, **3**, 280.
24 A. J. Lundeen and R. Van Hoozer, *J. Org. Chem.*, 1967, **32**, 3386.
25 J. F. Read, *Can. J. Chem.*, 1972, **50**, 490.
26 S. Brunauer, L. S. Deming, W. S. Deming, and E. Teller, *J. Am. Chem. Soc.*, 1940, **62**, 1723.
27 K. S. W. Sing, Proc. Int. Symp. Surface Area Determination, eds. D. H. Everett and R. H. Otterwill, Butterworths, London, 1970, p. 25.

*Received* 10*th June* 1982; *Paper* 2/979